

Tool influence functions of sapphire wheel polishing tools based on center supply polishing liquid

Chunliang Qi^{1,#}, Qingliang Zhao¹, Sheng Wang¹ and Jianbo Zhao¹

¹ Center for Precision Engineering, School of Mechatronics Engineering, Harbin Institute of Technology, Harbin, 150001, China

Corresponding Author / Email: qichunliang_cauc@163.com, TEL: +86-135-1200-3370, FAX: +86-0451-86415244

KEYWORDS: Sapphire, Wheel polishing, Polyurethane, Ultra-high molecular weight polyethylene, Tool influence function

Abstract: The precise tool influence function (TIF) of the polishing tool is crucial for polishing path planning. Therefore, designing polishing tool to ensure the central single peak removal feature of the TIF is of great practical significance. Firstly, this study designed a polyurethane polishing wheel and studied its fixed-point characteristics for polishing sapphire materials under different process parameters (rotational speed and compression offset) when external polishing fluid was supplied. Secondly, the material removal process of the polyurethane wheel and the shortcomings of the TIF characteristics were analyzed. A polyurethane wheel with a central supply of polishing fluid was proposed and fixed-point polishing was performed to verify its improvement in the TIF characteristics. Finally, further analysis and optimization were conducted, and an ultra-high molecular weight polyethylene (UHMWPE) polishing wheel based on central liquid supply was proposed. Fixed-point were performed to verify the stability of the UHMWPE polishing wheel in generating a central single peak removal function contour and the optimal process parameters.

1. Introduction

At present, the surface processing technology of sapphire optical components mainly relies on grinding, lapping, and polishing. Grinding or lapping is responsible for quickly removing a large amount of material to make the processed surface close to the target profile accuracy, and retaining a certain amount of machining allowance for subsequent polishing to the target precision surface. The high hardness, brittleness, and low fracture toughness of sapphire make it difficult to avoid introducing a certain degree of surface damage layer during grinding or lapping [1]. Therefore, subsequent polishing plays a crucial role in removing the surface damage layer and reducing surface roughness [2]. Facing the polishing of hard and brittle materials with various profile features, in order to achieve better material removal rate and profile convergence rate, contact sub-aperture polishing technology has gradually become the mainstream polishing form [3]. The research problems in the contact sub-aperture polishing process mainly focus on the precise control of the TIFs and the optimization of the polishing path based on the TIFs. The TIFs with Gaussian, quasi-Gaussian, or single peak removal profile features is a key advantage of polishing path planning. The combination of the two can optimize and improve the polishing quality and efficiency of optical components [4]. Therefore, it is of great practical significance to design a polishing tool to guarantee the central single-peak removal characteristic of its TIF.

Firstly, a contact semi-rigid polyurethane polishing wheel is designed. When the polishing liquid is supplied from the outside, the fixed-point polishing and groove polishing experiments are carried out on sapphire material under different process parameters such as polishing wheel speed and polyurethane compression offset. By analyzing the experimental results, the removal ability and removal quality of the polyurethane polishing wheel for polishing sapphire materials are studied. Then, analyzing the material removal process of the polyurethane wheel when the polishing liquid is supplied externally and the defects of the corresponding TIFs, and comparing the polyurethane wheel with the centrally supplied polishing liquid, and performing fixed-point polishing to verify that the form of the centrally supplied polishing liquid is in the material removal process and the TIFs improvement. Finally, the UHMWPE polishing wheel based on the central liquid supply is further analyzed and optimized. Fixed-point polishing and groove polishing experiments are performed to verify the ability and optimal process parameters of the UHMWPE wheel to produce single-peak TIFs in the center of the contact area.

2. TIFs of polyurethane polishing wheel

2.1 Semirigid polyurethane polishing wheel

As shown in Fig. 1, the polishing wheel structure in this chapter consists of an aluminum alloy substrate layer and a polyurethane polishing layer. The aluminum alloy substrate layer is the core support

part of the polishing tool, used to fix and support the polyurethane polishing layer to form a semirigid structure. The polyurethane polishing layer provides material removal power and has two important arc contour radii, namely a radial arc radius R of 25 mm and an axial arc radius r of 15 mm. The polyurethane polishing wheel has obvious independent pits and continuous peak surface features. The maximum radial height difference between the bottom of the pit and the peak surface is concentrated between 100 μm and 150 μm .

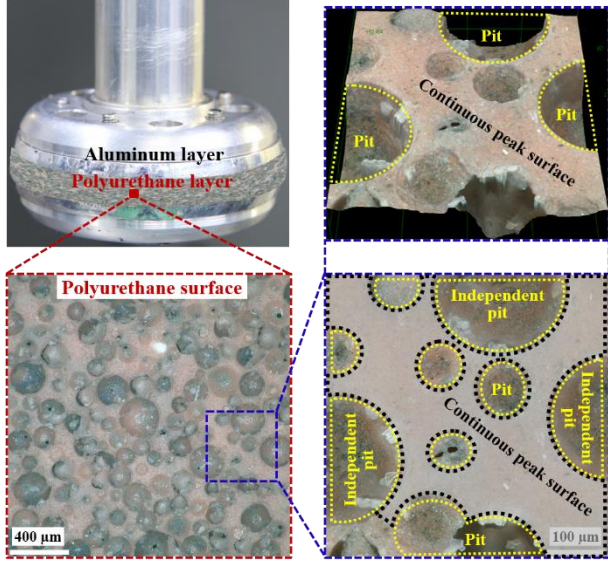


Fig. 1 Structure of polyurethane polishing wheel

2.2 Fixed-spot polishing

2.2.1 Experimental plan

The layout of the experimental device is shown in Fig. 2, and the system has the Kistler dynamometer and the acoustic emission sensor. The main function of acoustic emission sensors and the dynamometer is to precisely control the contact distance between the polishing wheel and the workpiece. The important process parameters in the fixed-spot polishing process are the polishing wheel speed n , the contact compression offset Δz between the polyurethane polishing layer and the workpiece, the polishing time Δt , polycrystalline diamond particle size d , and polishing fluid flow rate v . The complete polishing process parameters are shown in Table 1.

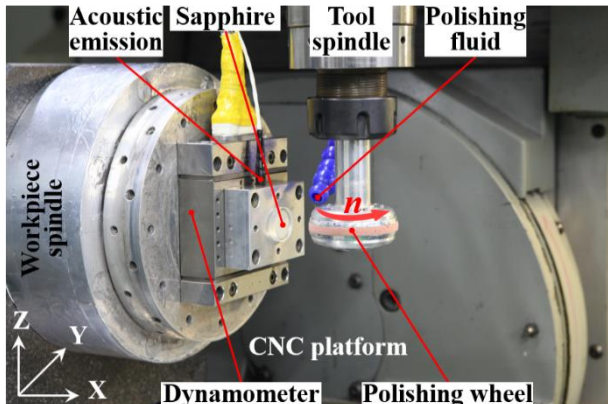


Fig. 2 Fixed-spot polishing experimental platform with external supply of polishing fluid

Table 1 Fixed-spot polishing process parameters

Parameter	Value
Wheel speed n/rpm	1000、1500、2000、2500、3000
Compression offset $\Delta z/\mu\text{m}$	100、150、200、250、300
Polishing time $\Delta t/\text{s}$	60
Particle size $d/\mu\text{m}$	1
Polishing fluid $v/\text{L}\cdot\text{min}^{-1}$	2
Workpiece material	Sapphire

2.2.1 Experimental results

The complete measurement results of the TIFs after fixed-point polishing under various process parameters are shown in Fig. 3. The TIFs of the polyurethane polishing wheel are all non-centrosymmetric distributions, that is, the positive center point of the theoretical contact area between the polyurethane layer and sapphire is not the deepest point of material removal depth, defined as non-contact center peak removal.

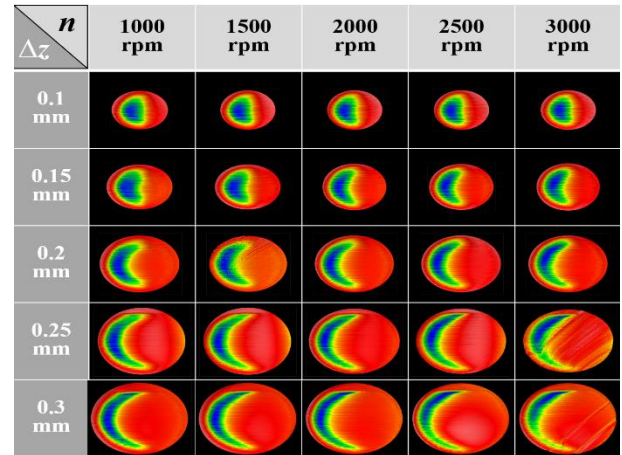


Fig. 3 The TIFs for fixed-point polishing

2.3 Material removal process and defect analysis

As shown in Fig. 4, a square area with a longitudinal dimension of 850 μm is extracted near the transverse centerline of the TIF. Further refinement can divide the entire square area into four main processing zones, namely the cutting-in zone A, peak zone B, stable zone C, and cutting-out zone D. As shown in Fig. 5, when diamond polishing particles enter the contact area between the polyurethane layer and sapphire, the division of the four regions is based on the number of polishing particles stored in the pit structure and the compression of polishing particles by peak characteristics.

As shown in Fig. 5, diamond polishing particles are sprayed towards the contact area through a high-pressure nozzle. When diamond polishing particles begin to enter the contact area, the polyurethane layer will store and bring the diamond polishing particles into the contact area through its surface micro pit structure. Immediately, under the squeezing effect of the polyurethane surface, diamond polishing particles began to remove the material. The cutting-in zone A is where diamond polishing particles begin to cut into the sapphire. As the polishing wheel continues to rotate, the diamond polishing particles are continuously removing the material. At the same time, the number of diamond polishing particles is continuously

decreasing, and when the number decreases to a certain extent, the depth of material removal begins to decrease and the amount of material removed also decreases accordingly. This stage is called the maximum cutting efficiency zone, namely peak zone B. As shown in Fig. 4, the material removal depth in peak region B also reaches its deepest point. As the polishing wheel continues to rotate, the squeezing effect of the surface begins to weaken, and the number of diamond polishing particles continues to decrease, resulting in a continuous decrease in material removal amount and depth. This stage is called the stable reduction zone of cutting efficiency, namely the stable zone C. Finally, the squeezing effect of the polyurethane surface gradually disappears, and the diamond polishing particles begin to slowly exit the contact area until the polishing particles no longer remove the material. This stage is called the cutting efficiency dissipation zone, also known as the cutting-out zone D. Therefore, in the case of external supply of polishing fluid, the TIF of polyurethane polishing wheel exhibits a transverse cross-sectional profile with non-centrosymmetric distribution, as well as a longitudinal cross-sectional profile with multiple peak removal features.

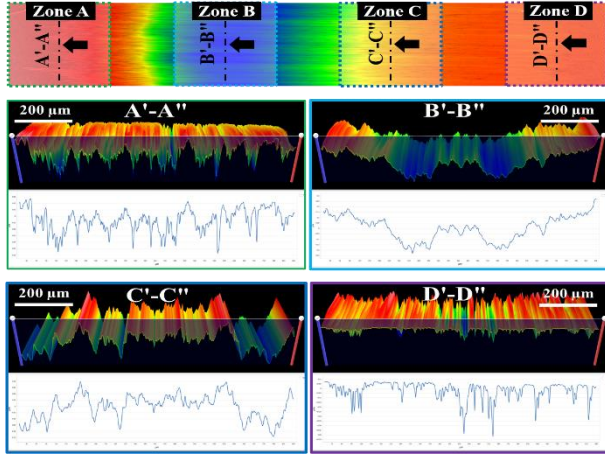


Fig. 4 Four key regions in the TIF

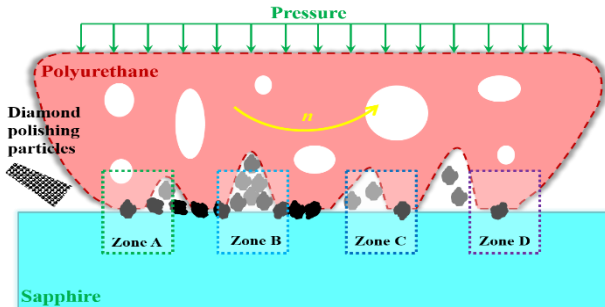


Fig. 5 Distribution of diamond polishing particles in the contact area

3. Polishing wheels based on centrifugal microchannel

3.1 Polyurethane polishing wheel

Therefore, in order to move the peak area towards the lateral center and increase the material removal in the stable zone, the supply mode of the polishing fluid is changed to increase the number of diamond polishing particles and their renewal efficiency in the peak and stable zones. As shown in Fig. 6, the polishing fluid is injected into the

centrifugal microchannel inside the polishing wheel at a certain pressure, and then the polishing particles diffuse along the spiral microchannel towards the outer circumference of the polishing wheel under the action of rotational centrifugal force. As shown in Fig. 7, the diamond polishing particles can effectively enter the contact area, thereby increasing and continuously updating the diamond polishing particles in the peak zone B and stable zone C.

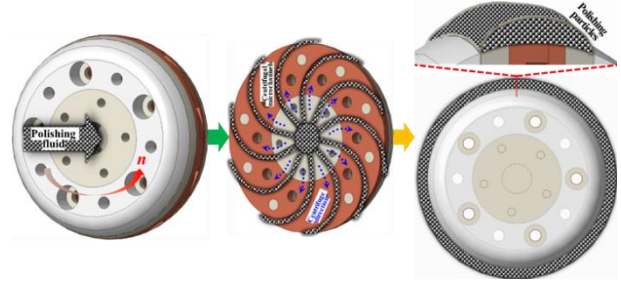


Fig. 6 The flow of polishing fluid under the action of centrifugal microchannels inside polyurethane polishing wheel

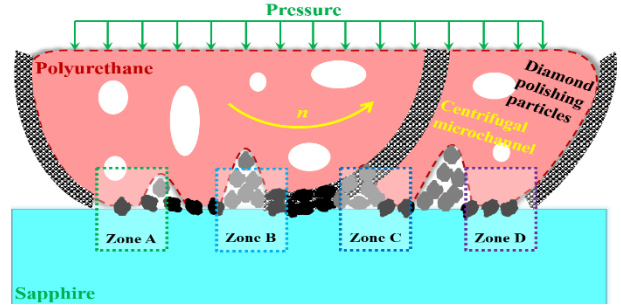


Fig. 7 Polishing fluid under the action of centrifugal microchannels

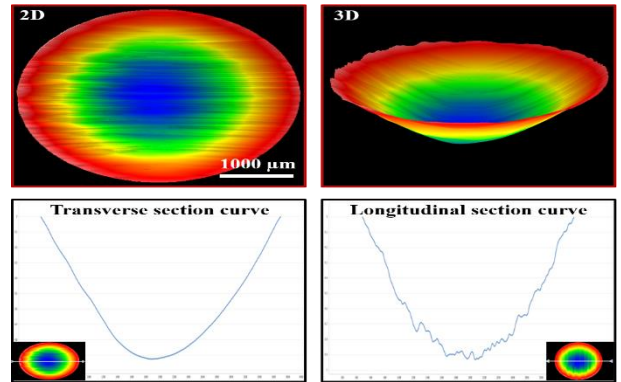


Fig. 8 The TIF characteristics of polyurethane polishing wheel

Perform fixed-point polishing on the improved polyurethane polishing wheel, with specific experimental parameters including a polishing wheel speed of 2000 rpm and a polyurethane compression offset of 100 μm . As shown in Fig. 8, the results indicate that the TIF has a transverse cross-sectional feature with a symmetrical distribution of contact centers, but the longitudinal cross-sectional profile feature still has a multi peak removal characteristic.

3.2 UHMWPE polishing wheel

The obvious surface fluctuations in the axial cross-sectional profile of the polyurethane polishing layer result in the longitudinal multi peak

removal feature of the TIF. Therefore, it is necessary to change the surface structure of the polishing layer to ensure that the polishing particles are evenly distributed in the longitudinal cross-sectional profile of the polishing layer. As shown in Fig. 9 and Fig. 10, compared to the high and low changes of several hundred micrometers on the surface of the polyurethane polishing layer, the UHMWPE in the form of woven fiber structure not only has an extremely delicate microstructure surface. The regular tiny gaps between fibers can also effectively constrain the diamond polishing particles to be distributed in a regular state along the longitudinal cross-section.

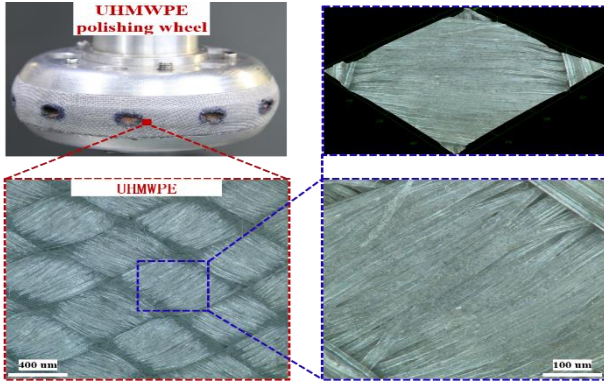


Fig. 9 UHMWPE polishing wheel

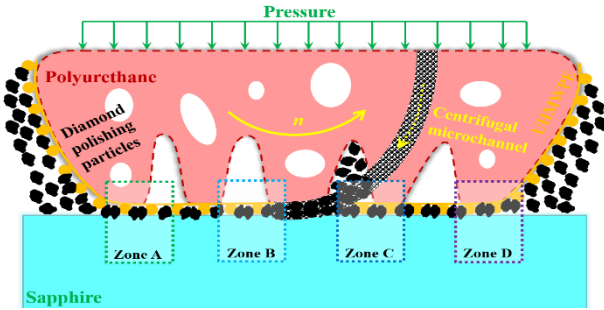


Fig. 10 Polishing particles between fibers in the contact area

The experimental platform for fixed-point polishing of UHMWPE polishing wheel with polishing fluid supplied at the center is shown in Fig. 3, and its specific process parameters are shown in Table 1. The TIFs of the UHMWPE polishing wheel is shown in Fig. 11 and Fig. 12, which demonstrate the longitudinal cross-sectional characteristics of the single peak distribution and the transverse cross-sectional characteristics of the center symmetric distribution in the TIF.

3. Conclusions

In the process of polishing sapphire materials with wheel polishing tools, optimizing the supply of polishing fluid can increase the number and renewal efficiency of polishing particles in key contact areas, thereby generating a transverse cross-sectional profile with a central symmetrical distribution. At the same time, by changing the microstructure characteristics of the polishing layer surface, the finer and more regularly distributed surface microstructure is more conducive to achieving single peak removal features. Compared to polyurethane polishing layers, UHMWPE polishing wheels based on central supply of polishing fluid can obtain the TIF of central single

peak removal.

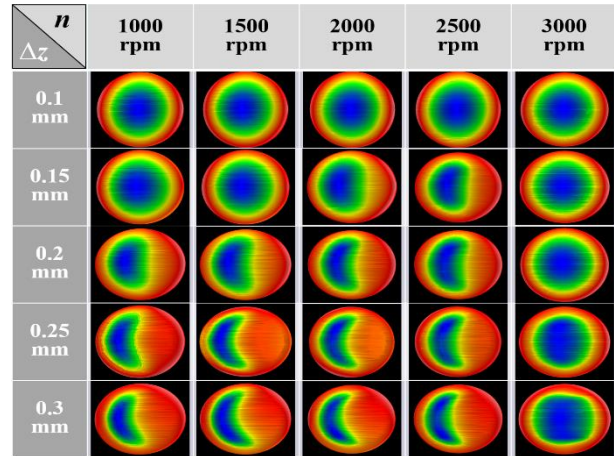


Fig. 11 The TIF characteristics of UHMWPE polishing

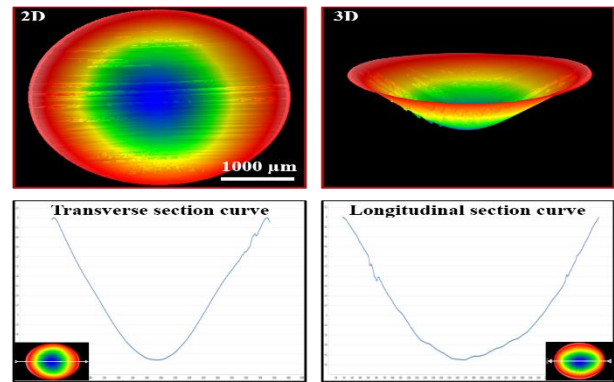


Fig. 12 The cross-sectional characteristics in the TIF.

ACKNOWLEDGEMENT

This work is supported by the National Natural Science Foundation of China [Grant No. 52305460].

REFERENCES

1. Zhang, L., Zhu, L., Zhou, T., Guo, P., Wang, X. and Liu, P., "Study on the Grinding Characteristics of Sapphire with the Assistant of Cerium Oxide Liquid," *Mater. Des.*, Vol. 215, 2022.
2. Gao, S., Li, H., Huang, H. and Kang, R., "Grinding and Lapping Induced Surface Integrity of Silicon Wafers and its Effect on Chemical Mechanical Polishing," *Appl. Surf. Sci.*, Vol. 599, 2022.
3. Guo, J., Beaucamp, A. and Ibaraki, S., "Virtual Pivot Alignment Method and its Influence to Profile Error in Bonnet Polishing," *Int. J. Mach. Tools Manuf.*, Vol. 122, pp. 18-31, 2017.
4. Jiannan, Z., Zhong-Chen, C., Junpeng, Z., Chenyao, Z. and Haitao, L., "Development and Theoretical Analysis of Novel Surface Adaptive Polishing Process for High-efficiency Polishing of Optical Freeform Surface," *J. Manuf. Process.*, Vol. 80, pp. 874-886, 2022.